ChemComm

COMMUNICATION

View Article Online
View Journal | View Issue

Cite this: *Chem. Commun.*, 2024, **60**, 1727

Received 9th October 2023,
Accepted 10th January 2024

DOI: 10.1039/d3cc04948e

rsc.li/chemcomm

An esterase-cleavable persulfide donor with no electrophilic byproducts and a fluorescence reporter†

Bharat S. Choudhary, ‡[a] T. Anand Kumar, ‡[a] Akshi Vashishtha, [b] Sushma Tejasri, [a] Amal S. Kumar, [a] Rachit Agarwal [b] and Harinath Chakrapani *[a]

Hydrogen sulfide (H_2S) and associated sulfur species known as persulfide or sulfane sulfur are considered among the first responders to oxidative stress. However, tools that reliably generate these species without any potentially toxic byproducts are limited, and even fewer report the generation of a persulfide. Here, using a latent fluorophore embedded with *N*-acetylcysteine persulfide, we report a new tool that is cleaved by esterase to produce a persulfide as well as a fluorescence reporter without any electrophilic byproducts. The rate of formation of the fluorescence reporter is nearly identical to the rate of formation of the persulfide suggesting that the use of this probe eliminates the need for secondary assays that report persulfide formation. Symptomatic with persulfide generation, the newly developed donor was able to protect chondrocyte cells from oxidative stress.

The gasotransmitter hydrogen sulfide (H_2S) has emerged as an important mediator of numerous cellular processes and a possible therapeutic agent in a number of diseases including progressive degenerative diseases associated with inflammation such as Parkinson's, Alzheimer's and osteoarthritis.[1–4] Recently, an oxidative post-translation modification induced by H_2S, known as protein persulfidation[4–6] where a cysteine (RSH) is modified to a persulfide (RS-SH), has been shown to have protective effects in cells under oxidative stress.[7] For example, KEAP1 an oxidative stress sensor protein forms a complex with Nrf2 under normal conditions, where Nrf2 is ubiquitinated by the Culin3-KEAP1 E3 ubiquitin ligase complex leading to proteasomal degradation. Under oxidative stress conditions, persulfidation of KEAP1 leads to the dissociation of the KEAP1-Nrf2 complex. The liberated Nrf2 then translocates to the nucleus and promotes the activation of antioxidant responsive elements (AREs).[8–10] While many tools have been developed to reliably generate persulfides, including those activated by enzymes,[11–15] light,[16,17] reactive oxygen species (ROS),[18–21] pH,[22,23] fluoride[22] and peroxynitrite.[24] One possible limitation with some of these approaches is the generation of electrophilic byproducts such as a quinone methide[13,14,18,21,24] or an aldehyde;[11,16,17,20] such byproducts may contribute to electrophilic stress.[25,26] Also, there is a need for secondary assays to report persulfide produced by these donors. To overcome the need for secondary assays to report persulfide generation, a latent fluorophore strategy can be employed. Upon activation by particular stimuli, the protective group gets cleaved (Step 1) leading to the formation of an intermediate, which subsequently dissociates (Step 2) to release persulfide along with a fluorescence reporter (Fig. 1a).

Recently, a donor that generates persulfide (H_2S_2) as well as a fluorescence reporter upon activation by light were reported (Fig. 1b).[17] However, the applicability of this tool may be limited by the generation of electrophilic byproducts as well as the limited use of light-based tools in the cellular experiments. Here, we developed a tool that generates persulfide along with a fluorophore that reports the generation of persulfide.

To achieve this goal, we considered lactonization as the key step in persulfide generation (Fig. 1c). Hence, a biphenyl-based system was chosen here, cleavage of the ester by esterase (Es) should lead to lactonization, which generates a lactone that belongs to a class of known fluorophores.[27,28] Lactonization in such systems is reported to be quite rapid;[29] hence, the persulfide generation will likely occur during lactonization leading to nearly concomitant release of the persulfide and the production of a fluorescence signal.

Compound **2a** (Scheme 1) was synthesized following a reported protocol.[30] Reduction of lactone by LAH, silyl protection of the resulting alcohol, and esterification with cyclopropyl carboxylic acid (CPCA) followed by silyl group deprotection afforded compound **6**.

[a] *Department of Chemistry, Indian Institute of Science Education and Research Pune, Pune 411 008, Maharashtra, India. E-mail: harinath@iiserpune.ac.in*
[b] *Department of Bioengineering, Indian Institute of Science, Bengaluru 560 012, Karnataka, India*

† Electronic supplementary information (ESI) available. See DOI: https://doi.org/10.1039/d3cc04948e

‡ These authors contributed equally.

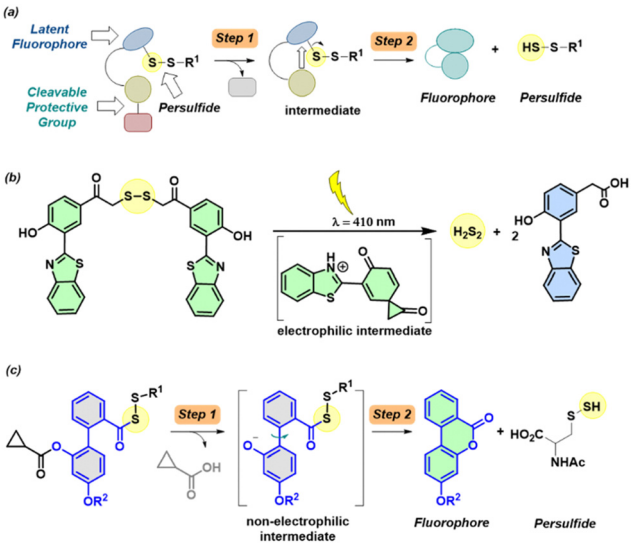

Fig. 1 (a) General design for a cleavable persulfide donor with a fluorescence reporter. The first step is the cleavage of the protective group, which produces an intermediate that is then converted to a fluorophore and produces persulfide as a byproduct. (b) Light activated H_2S_2 donor with a fluorescence reporter. (c) Proposed biphenyl-system that is cleaved by esterase to produce a phenolate intermediate that cyclizes to produce a lactone that is fluorescent and persulfide.

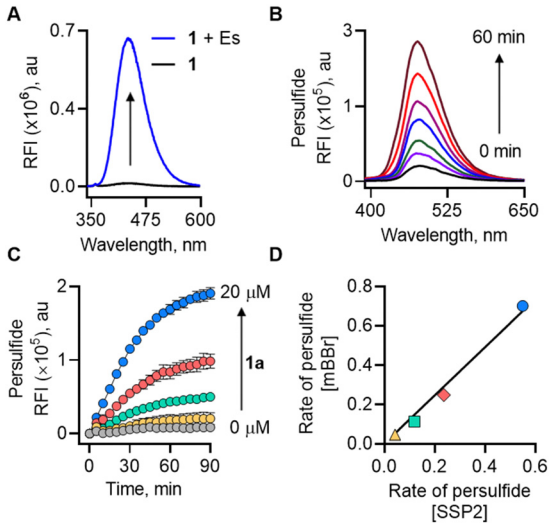

Fig. 2 (A) Monitoring the formation of lactone (**2a**) from **1** by fluorescence at 20 μM without or with Es (1 U mL^{-1}) in pH 7.4 buffer at 37 °C. (B) Detection of persulfide released from **1** (100 μM) upon treatment with Es (1 U mL^{-1}) and mBBr (100 μM) over 60 min. (C) Monitoring the release of persulfide generated upon co-treatment of Es (1 U mL^{-1}) and SSP2 (10 μM) with varied concentrations of **1** (0–20 μM) over 90 min. (D) Correlation between the rate of persulfide formation from **1** (△ 2.5 μM; □ 5 μM; ◇ 10 μM and ○ 20 μM) in mBBr and SSP2 assays.

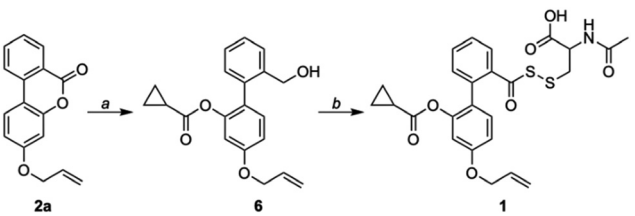

Scheme 1 Synthesis of **1**: (a) (i) LAH, THF, 0 °C; (ii) TBDMSCl, Imh, RT; (iii) CPCA, DCC, DMAP, RT; (iv) AcOH, THF:H_2O, RT; (b) (i) PCC, DCM, RT; (ii) KH_2PO_4, H_2O_2, $NaClO_2$, DCM, RT; (iii) Lawesson's reagent, toluene, 120 °C; (iv) **9** (NAC-SS-Py), $CHCl_3$, RT.

Oxidation of a primary alcohol in two steps gave carboxylic acid **8**, which was then converted to its corresponding thiocarboxylic acid using Lawesson's reagent and finally coupled with NAC-pyridyl disulfide (NAC-SS-Py) **9** to provide the persulfide donor **1** (Scheme S1, ESI†). This compound with an allyl group was used for initial experiments, since the lactone (**2b**) without the allyl group had diminished fluorescence signal when compared with **2a** (see ESI,† Fig. S1). We hence proceeded to use **1** which has an allyl group for our analysis.

We first examined the formation of lactone (**2a**) from **1** (20 μM) by monitoring the change in fluorescence in the presence of Es (1 U mL^{-1}). The compound was itself non-fluorescent, but addition of Es (1 U mL^{-1}) led to a significant increase in fluorescence intensity (48-fold) attributable to the formation of **2a** (λ_{ex} = 320 nm; λ_{em} = 432 nm;) after incubation for 1 h in pH 7.4 buffer (Fig. 2a). The formation of **2a** was independently confirmed by mass spectrometry analysis (m/z 253.0864; see ESI,† Fig. S2). Furthermore, dose-dependent studies demonstrated that the fluorescence gradually increased over time and plateaued after 1 h (see ESI,† Fig. S3). Curve fitting for lactone formation to a first-order exponential equation yielded rate constants ranging from 0.046 to 0.073 min^{-1} (see ESI,† Table S1). These results supported that **1** underwent lactonization to produce **2a** following esterase-mediated hydrolysis. We tested the ability of **1** to be cleaved under cell culture conditions and found that **1** was cleaved in cell lysates to produce a fluorescence signal (see ESI,† Fig. S4). Compound **1** was well tolerated by MEF cells up to 100 μM (see ESI,† Fig. S5). To ascertain if **1** permeates cells to generate **2a**, MEF cells were treated with **1** followed by confocal imaging after 4 h, since this class of fluorophores is known to be compatible with two-photon imaging[31] (λ_{ex} = 700 nm; see ESI,† Fig. S6). Together, these results support the suitability of **1** in cellular assays.

Next, a series of experiments were conducted to directly trap the persulfide release from **1** using electrophilic trapping agents and persulfide-specific fluorescent probes. First, a monobromobimane (mBBr)-based fluorescence enhancement assay was used.[17] Here, when **1** was co-incubated with Es and mBBr, we found a distinct time-dependent increase in fluorescence (λ_{ex} = 380 nm; λ_{em} = 455 nm) (Fig. 2b). This fluorescence was attributed to the formation of **NAC-SS-bimane** adduct ($M + Na^+$; m/z 408.0663) (Scheme S2, ESI†), which was further confirmed by MS analysis (see ESI,† Fig. S7). A dose-dependent study of **1** with mBBr showed a good linear relationship (see ESI,† Fig. S8).

Independently, we also measured the rate of persulfide generation from **1** using a well-established fluorogenic probe,

sulfane sulfur probe (SSP2).[32] Again, we observed a significant increase in fluorescence intensity (λ_{ex} = 482 nm; λ_{em} = 518 nm), corresponding to the generation of sulfane sulfur (Fig. 2c). Under these experimental conditions, the rate of persulfide formation in both mBBr and SSP2 assays showed an excellent correlation (R^2 = 0.99) (Fig. 2d).

The time course for the formation of **2a** as well as NAC persulfide at various concentrations of **1** was independently monitored by the change in fluorescence signal. When followed over 90 min, the time courses of these events were similar. The rate for lactone formation was found to be marginally higher in magnitude (2–3 fold) than the rate of persulfide generation (see ESI,† Table S1). This is expected since the lactonization occurs at a faster rate compared to the rate of formation of NAC persulfide covalent adducts that occurs through a two-step process rather than a single step. To establish a correlation between the lactone (**2a**) and persulfide formation (SSP2) from **1**, the maximum fluorescence change at 90 min was considered as the plateau was reached. These values were normalized and then plotted. An excellent correlation between the two parameters was observed, suggesting that the release of fluorophore and NAC persulfide occurs nearly concurrently following esterase-mediated cleavage and subsequent lactonization (Fig. 3a). Similarly, the rates of persulfide generation as determined by SSP2 and rates of lactone **2a** formation showed a good linear relationship at concentrations ranging from 2.5 to 20 μM (Fig. 3b). Taken together, these data show that the fluorescence signal produced can be used as a proxy for persulfide production.

Lastly, two additional assays were carried out to demonstrate persulfide and hydrogen sulfide formation. A standard LC/MS assay was conducted using an established **HPE-IAM** electrophile as a persulfide trapping agent (Scheme S3, ESI†).[33] Upon co-incubation of **1** in the presence of Es (1 U mL^{-1}) and **HPE-IAM**, a new peak attributable to a persulfide adduct, **NAC-SS-HPE-AM** (*m*/*z* 373.0891), was observed, indicating the release of NAC persulfide (see ESI,† Fig. S9 and S10). Under these conditions, we also observe **Bis-*S*-HPE-AM** (*m*/*z* 389.1537), presumably due to the reaction of HPE-IAM with H_2S formed by the decomposition of NAC persulfide through disproportionation (see ESI,† Fig. S9 and S11). Lastly, we measured H_2S formation from **1** using the standard methylene blue (MB) colorimetric assay.[34] This assay revealed the formation of H_2S from **1** in the presence of Es and excess amounts of DTT (see ESI,† Fig. S12). To independently verify H_2S release, we employed a lead acetate assay. Addition of an aliquot of the reaction mixture containing **1** and Es to lead acetate paper resulted in a dark coloration, indicating the formation of lead sulfide (see ESI,† Fig. S13).

Osteoarthritis (OA) is the most common joint disease and is characterized by a gradual loss of articular cartilage and joint hypertrophy.[35] Chronic inflammation and oxidative stress contribute to the onset and progression of OA.[36,37] We considered the antioxidant property of persulfide as a possible therapeutic strategy to alleviate oxidative stress and inflammation in chondrocytes. Persulfides are known to exhibit potent antioxidant properties, superior to thiols and H_2S against oxidative stress.[7] We first measured the cytotoxicity of **1** in the human chondrocyte C28/I2 cells and found that the compound was well tolerated up to 50 μM and the LD50 was found to be ~500 μM (Fig. 4a and see ESI,† Fig. S14). This result is consistent with no electrophilic byproducts being formed during the persulfide generation step. Next, we determined the cytoprotective effects of **1** in C28/I2 cells against oxidative stress induced by a cell-permeable ROS generator MGR-1 (Scheme S4, ESI†).[38] Cells were preincubated with **1** for 3 h and then were exposed to MGR-1 (15 μM), after which cell viability was assessed. As expected, exposure of cells to MGR-1 resulted in a drastic reduction in cell viability. Pre-treatment of cells with **1** demonstrated significant protective effects from MGR-1 induced oxidative stress in a concentration-dependent manner (Fig. 4b). A similar result was recorded when **1** was co-treated with MGR-1 or added after exposure to MGR-1 (see ESI,† Fig. S15). To understand if **1** acted through diminishing ROS levels, a standard H_2-DCFDA assay was performed in MEF cells (see ESI,† Fig. S16). These results indicate that **1** was capable of protecting as well as rescuing cells from oxidative stress.

The central characteristic of osteoarthritis (OA) is the degradation of the extracellular matrix (ECM). When chondrocytes are densely seeded (micromass) and exposed to specific growth factors, they release extracellular matrix (ECM) components,

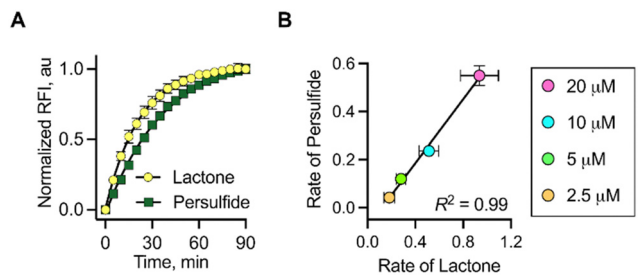

Fig. 3 (A) Correlation between change in fluorescence corresponding to the formation of lactone and persulfide formed upon incubation of **1** (20 μM) with Es (1 U mL^{-1}) and SSP2 (10 μM). (B) Correlation between the rates of lactone and persulfide formation upon treatment of **1** (2.5, 5, 10 and 20 μM) with Es (1 U mL^{-1}) in the presence of SSP2 (10 μM).

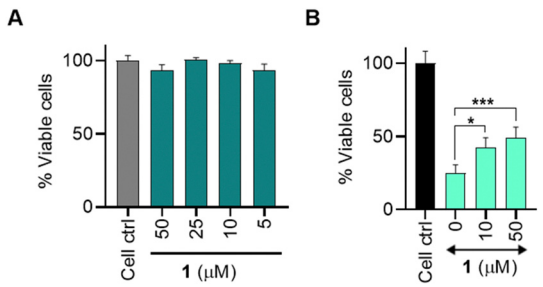

Fig. 4 A cell viability assay conducted on C28/I2 cells. (A) Cells treated with varying concentrations of compound **1** for 24 h. (B) Cells treated with varying concentration of **1** followed by treatment with MGR-1 (15 μM). All data are presented as mean ± SD (*n* = 4/group). Statistical significance was established relative to MGR-1 using one-way ANOVA (*$p < 0.033$, ***$p \leq 0.001$).

such as sulphated glycosaminoglycans (sGAG).[39] Next, we employed micromass cultures derived from the C28/I2 cell line,[40,41] which can be considered as an *in vitro* mimic of the cartilage[39,41] to assess the ability of **1** in sustaining sGAG production in the presence of oxidative stress induced by MGR-1. sGAG production was measured using Alcian blue staining as described.[39–41] When exposed to MGR-1 alone, there was a significant decrease in absorbance compared to the untreated group. However, micromasses co-treated with MGR-1 and **1** displayed an increased absorbance, similar to the untreated samples, indicating that the cells were capable of sustaining sGAG production even under oxidative stress when co-treated with **1** (see ESI,† Fig. S17). These results support the ability of persulfides generated by **1** to counter oxidative stress in a model relevant to OA. Further *in vitro* and *in vivo* experiments towards exploiting the therapeutic potential of persulfide generating systems for the treatment of OA are indicated.

In summary, we report a new probe that is cleaved by esterase to produce persulfide as well as a fluorescence signal. No electrophilic byproducts were formed during this reaction (see ESI,† Fig. S18), and the rate of persulfide generation closely correlated with the rate of generation of a fluorescence signal. Hence, the use of this new tool eliminates the need for independent assays to detect persulfides.

Financial support was provided by the Science and Engineering Research Board (CRG/2019/002900), Department of Biotechnology (HC, BH/HRD/NBM-NWB/39/2020-21) and IISER Pune, and the DST Fund for Improvement of S&T Infrastructure (SR/FST/LSII-043/2016) to the IISER Pune Biology Department for setting up the Biological Mass Spectrometry Facility. The manuscript was written with inputs from all authors. BSC, TAK, AV, ST and ASK carried out all experiments under the supervision of RA and HC.

Conflicts of interest

There are no conflicts to declare.

Notes and references

1 T. V. Mishanina, M. Libiad and R. Banerjee, *Nat. Chem. Biol.*, 2015, **11**, 457–464.
2 M. R. Filipovic, J. Zivanovic, B. Alvarez and R. Banerjee, *Chem. Rev.*, 2018, **118**, 1253–1337.
3 S. Nasi, D. Ehirchiou, A. Chatzianastasiou, N. Nagahara, A. Papapetropoulos, J. Bertrand, G. Cirino, A. So and N. Busso, *Arthritis Res. Ther.*, 2020, **22**, 49.
4 A. K. Mustafa, M. M. Gadalla, N. Sen, S. Kim, W. Mu, S. K. Gazi, R. K. Barrow, G. Yang, R. Wang and S. H. Snyder, *Sci. Signaling*, 2009, **2**, ra72.
5 C. Yang, N. O. Devarie-Baez, A. Hamsath, X. Fu and M. Xian, *Antioxid. Redox Signaling*, 2020, **33**, 1092–1114.
6 H. Kimura, *Br. J. Pharmacol.*, 2020, **177**, 720–733.
7 T. Ida, T. Sawa, H. Ihara, Y. Tsuchiya, Y. Watanabe, Y. Kumagai, M. Suematsu, H. Motohashi, S. Fujii, T. Matsunaga, M. Yamamoto, K. Ono, N. O. Devarie-Baez, M. Xian, J. M. Fukuto and T. Akaike, *Proc. Natl. Acad. Sci. U. S. A.*, 2014, **111**, 7606–7611.
8 J. W. Kaspar, S. K. Niture and A. K. Jaiswal, *Free Radical Biol. Med.*, 2009, **47**, 1304–1309.
9 S. Koike, Y. Ogasawara, N. Shibuya, H. Kimura and K. Ishii, *FEBS Lett.*, 2013, **587**, 3548–3555.
10 G. Yang, K. Zhao, Y. Ju, S. Mani, Q. Cao, S. Puukila, N. Khaper, L. Wu and R. Wang, *Antioxid. Redox Signaling*, 2013, **18**, 1906–1919.
11 Y. Zheng, B. Yu, Z. Li, Z. Yuan, C. L. Organ, R. K. Trivedi, S. Wang, D. J. Lefer and B. Wang, *Angew. Chem., Int. Ed.*, 2017, **56**, 11749–11753.
12 Z. Yuan, Y. Zheng, B. Yu, S. Wang, X. Yang and B. Wang, *Org. Lett.*, 2018, **20**, 6364–6367.
13 K. M. Dillon, R. J. Carrazzone, Y. Wang, C. R. Powell and J. B. Matson, *ACS Macro Lett.*, 2020, **9**, 606–612.
14 K. M. Dillon, H. A. Morrison, C. R. Powell, R. J. Carrazzone, V. M. Ringel-Scaia, E. W. Winckler, R. M. Council-Troche, I. C. Allen and J. B. Matson, *Angew. Chem., Int. Ed.*, 2021, **60**, 6061–6067.
15 P. Bora, M. B. Sathian and H. Chakrapani, *Chem. Commun.*, 2022, **58**, 2987–2990.
16 A. Chaudhuri, Y. Venkatesh, J. Das, M. Gangopadhyay, T. K. Maiti and N. D. P. Singh, *J. Org. Chem.*, 2019, **84**, 11441–11449.
17 A. Chaudhuri, Y. Venkatesh, B. C. Jena, K. K. Behara, M. Mandal and N. D. P. Singh, *Org. Biomol. Chem.*, 2019, **17**, 8800–8805.
18 C. R. Powell, K. M. Dillon, Y. Wang, R. J. Carrazzone and J. B. Matson, *Angew. Chem., Int. Ed.*, 2018, **57**, 6324–6328.
19 R. A. Hankins, S. I. Suarez, M. A. Kalk, N. M. Green, M. N. Harty and J. C. Lukesh, *Angew. Chem., Int. Ed.*, 2020, **59**, 22238–22245.
20 P. Bora, P. Chauhan, S. Manna and H. Chakrapani, *Org. Lett.*, 2018, **20**, 7916–7920.
21 Y. Wang, K. M. Dillon, Z. Li, E. W. Winckler and J. B. Matson, *Angew. Chem., Int. Ed.*, 2020, **59**, 16698–16704.
22 J. Kang, S. Xu, M. N. Radford, W. Zhang, S. S. Kelly, J. J. Day and M. Xian, *Angew. Chem., Int. Ed.*, 2018, **57**, 5893–5897.
23 V. S. Khodade, B. M. Pharoah, N. Paolocci and J. P. Toscano, *J. Am. Chem. Soc.*, 2020, **142**, 4309–4316.
24 Y. Xu, B. Xu, J. Wang, H. Jin, S. Xu, G. Wang and L. Zhen, *Chem. – Eur. J.*, 2022, **28**, e202200540.
25 D. C. Thompson, J. A. Thompson, M. Sugumaran and P. Moldéus, *Chem. – Biol. Interact.*, 1993, **86**, 129–162.
26 K. Ali, P. Mishra, A. Kumar, D. N. Reddy, S. Chowdhury and G. Panda, *Chem. Commun.*, 2022, **58**, 6160–6175.
27 A. Fallah, B. Noshadi, M. Gazi and H. O. Gülcan, *J. Fluoresc.*, 2020, **30**, 113–120.
28 X. Peng, J. Gao, Y. Yuan, H. Liu, W. Lei, S. Li, J. Zhang and S. Wang, *Bioconjugate Chem.*, 2019, **30**, 2828–2843.
29 M. Caswell and G. L. Schmir, *J. Am. Chem. Soc.*, 1980, **102**, 4815–4821.
30 A. T. Franks and K. J. Franz, *Chem. Commun.*, 2014, **50**, 11317–11320.
31 P. D. McFadden, K. Frederick, L. A. Argüello, Y. Zhang, P. Vandiver, N. Odegaard and D. A. Loy, *ACS Appl. Mater. Interfaces*, 2017, **9**, 10061–10068.
32 W. Chen, C. Liu, B. Peng, Y. Zhao, A. Pacheco and M. Xian, *Chem. Sci.*, 2013, **4**, 2892–2896.
33 H. A. Hamid, A. Tanaka, T. Ida, A. Nishimura, T. Matsunaga, S. Fujii, M. Morita, T. Sawa, J. M. Fukuto, P. Nagy, R. Tsutsumi, H. Motohashi, H. Ihara and T. Akaike, *Redox Biol.*, 2019, **21**, 101096.
34 A. K. Sharma, M. Nair, P. Chauhan, K. Gupta, D. K. Saini and H. Chakrapani, *Org. Lett.*, 2017, **19**, 4822–4825.
35 J. Martel-Pelletier, *Osteoarthr. Cartil.*, 1998, **6**, 374–376.
36 M. Y. Ansari, N. Ahmad and T. M. Haqqi, *Biomed. Pharmacother.*, 2020, **129**, 110452.
37 L. Liu, P. Luo, M. Yang, J. Wang, W. Hou and P. Xu, *Front. Mol. Biosci.*, 2022, **9**, 1001212.
38 D. S. Kelkar, G. Ravikumar, N. Mehendale, S. Singh, A. Joshi, A. K. Sharma, A. Mhetre, A. Rajendran, H. Chakrapani and S. S. Kamat, *Nat. Chem. Biol.*, 2019, **15**, 169–178.
39 K. V. Greco, A. J. Iqbal, L. Rattazzi, G. Nalesso, N. Moradi-Bidhendi, A. R. Moore, M. B. Goldring, F. Dell'Accio and M. Perretti, *Biochem. Pharmacol.*, 2011, **82**, 1919–1929.
40 K. M. Dhanabalan, A. A. Dravid, S. Agarwal, R. K. Sharath, A. K. Padmanabhan and R. Agarwal, *Bioeng. Transl. Med.*, 2023, **8**, e10298.
41 C. De Bari, F. Dell'Accio and F. P. Luyten, *Arthritis Rheum.*, 2001, **44**, 85–95.

